Cold sprayability of mixed commercial purity Ti Plus Ti6Al4V metal powders

Aydin, Huseyin; Alomair, Mashael; Wong, Wilson; Vo, Phuong; Yue, Stephen

Publisher's version / Version de l'éditeur:
https://doi.org/10.1007/s11666-017-0528-7
Journal of Thermal Spray Technology, 2017-01-30

Cold Sprayability of Mixed Commercial Purity (CP)-Ti plusTi6Al4V Metal Powders

Huseyin AYDIN[1], Mashael ALOMAIR[1], Wilson WONG[1], Phuong Vo[2] and Stephen YUE[1]

[1]McGill University; Department of Mining and Materials Engineering; Montreal, QC, Canada

[2]National Research Council, Boucherville, Quebec, Canada

Corresponding author: E-mail address: huseyin.aydin@mail.mcgill.ca

Submitted to

May 2016

Abstract

In the present work, metallic composite coatings of commercial purity CP-Ti plus Ti6Al4V were produced by cold spraying to explore the effect of mixing on porosity and mechanical properties of the coatings. The coatings were deposited using N_2 gas at 800 °C and 4 MPa pressure on 1020 steel substrate. Coating characteristics were studied by examining porosity percentages and Vickers's hardness. The microstructure was examined using optical and electron microscopy techniques. It was observed that mixing metal powders can lead to improvements in cold sprayability (i.e. increases in the deposition efficiency and decreases in the porosity) of the 'matrix' powder. It is shown that a critical addition can significantly influence cold sprayability, but above this critical level, there is little change in cold sprayability. Hardness differences between the two powders are considered to be the first order influence, but differences in particle sizes and morphology may also be contributing factors.

Keywords: Cold Spray, Mixed Metal Powders Coating, Deposition Efficiency, Porosity

1. Introduction

Over the last few years, cold gas dynamic spraying which is an important part of the thermal spray coating family has become an emerging manufacturing and repair technology, particularly in the aerospace industry. This technique enables production of various coatings, such as pure metals, alloys, composites, nanostructure materials, and even amorphous materials. It is an all-solid state, high kinetic energy, coating and free-form fabrication process that uses high pressure compressed gas to propel solid particles of diameters between 20 and 50 μm onto a substrate under atmospheric conditions (Ref 1,2).

In general, for a given set of powder characteristics (i.e. composition, microstructure, and morphology, size and size distribution) and substrate combination, increasing the spray process intensity (i.e. the gas temperature and pressure) will definitely increase the DE and possibly decrease the porosity, primarily because the particle velocity is increased (Ref 2-5). However, cold sprayed pure titanium and Ti6Al4V coatings are reported to be quite porous even at very high particle velocities, although deposition efficiencies are close to 100% (Ref 6,7).

In the cold spray literature, there are many examples of mixing metal powders with ceramic powders (Ref 8-10), which illustrates the main reason for mixing powders – creating materials with improved or novel properties. There is, however, comparatively limited work concerning mixed metal powders that are subsequently cold spray, but the few examples of consolidating mixed metal powders by cold spray are also centered on producing materials with novel properties. For example, Al-Mangour et.al mixed powders to produce a composite with controlled micro galvanic corrosion behavior for use as a biodegradable stent (Ref 11).

However, there are other circumstances that justify mixing powders. For example, if there is a limited supply of an expensive or experimental metal alloy in powder form, then mixing with a

readily available powder, preferably of similar characteristics, will give some limited knowledge of the cold sprayability of the powder. More fundamentally, observing the cold spray characteristics of two metal powders with different characteristics can lead to a better understanding of the mechanisms of cold spray deposition and consolidation. In other words, mixing powders can lead to interesting (i.e. unexpected) effects on deposition efficiency, porosity and even post cold spray annealing behavior. For example, there are studies showing that adding ceramic powders to metal powders can decrease porosity (Ref 8-10). Of course, this technique is only of use if the presence of the ceramic powder in the coating does not adversely affect the other relevant coating properties. This paper explores the possibility of decreasing porosity by adding a metal powder rather than a ceramic.

In this study CP-Ti and Ti6Al4V powders were mixed in different proportions and cold sprayed using nitrogen as propellant gas. Firstly, the effect on deposition efficiency, and the coating porosity, hardness and flow behavior is detailed. Then, the evolution of the mechanical properties before and after post heat treatment conditions is discussed.

2. Experimental Methods

2.1. Feedstock Powder

The two feedstock powders are of commercially available plasma-atomised grade 1 spherical CP-Ti (-29+15 μm) and spherical Ti6Al4V (-29+15 μm) powders manufactured by Raymor (Montreal, Canada); their chemical compositions are given in **Table 1**. As can be seen from the spherical morphology (**Fig. 1**), both powders were processed by plasma atomization. In the case of mixed powders, the mixing was performed in a ball mill prior to spraying. Analysis of the

feedstock powder revealed that the average microhardness for CP-Ti was 141 ± 10 HV_{10} and for Ti6Al4V 385 ± 10 HV_{10}.

2.2. Cold Spray Parameters and Diagnostics

The cold spray system used to produce the coatings was a KINETIKS® 4000 (CGT-GmbH, Ampfing, Germany). Nitrogen was used as the propellant gas with a CGT MOC24 nozzle; the key process parameters are given in **Table 2**. The temperature and pressure are the maximum for this gun and the other parameters are typical for cold spray. Particle velocity was measured in free jet using an optical time-of-flight diagnostic tool (Cold Spray Meter, Tecnar Automation, St. Bruno, QC, Canada) (Ref 12); the average particle velocity was 710 ± 10 m/s.

The powders were cold sprayed onto grit-blasted, 1020 steel plates (76 × 76 × 3 mm) to obtain a nominal coating thickness of 2 mm. These coupons were degreased with alcohol and grit blasted prior to spraying. Following deposition, an ISOMET diamond saw was employed to separate the deposited material from the substrate and all subsequent testing and microstructural analysis was performed on the coating only.

2.3. Heat Treatment

Post-spray processing consisted of annealing at 600°C for 30 min in an argon atmosphere.

2.4. Microstructural Characterization

Samples were sectioned perpendicular to the spray direction, hot mounted in resin and mechanically ground and polished using standard metallographic preparation procedures. An aqueous solution of 45 mL HCl, 15 mL HNO_3 and 20 mL methanol was used for etching. A

Clemex optical microscope and a field emission-scanning electron microscope (Philips XL30 FEG-SEM) were used to characterize the powder and coatings. The porosity was measured from the cross sections of the coatings using image analysis (Clemex Vision, Clemex Technologies Inc., Longueuil, QC) on a minimum of 10 random fields obtained using both optical microscopy and SEM backscattered electron mode (BSE) at 500× magnification.

2.5. Mechanical Testing

The coating hardness was measured using a Vickers tester (Clark CM100AT, SUN-TEC Corp., Novi, USA) at a load of 1 kg for a minimum of 10 measurements taken at random locations on both polished and etched cross section of coatings. Shear punch tests were performed on a MTS 810 (MTS Systems Corp., Eden Prairie, USA) at room temperature and a strain rate of 10^{-2} s^{-1}. Specimen deformation was assumed to be equal to the crosshead displacement and therefore load-displacement measurements were used to study the plastic flow behaviour. Shear punch samples were polished to make the specimen surfaces consistent. Figure 2 schematically illustrates a shear punch testing machine. A load cell is located in the lower testing bed, and the displacement can be measured by one of the laser displacement meter and strain gauges. The most important characteristic of this test is that the absorbed energy, testing speed, and strain rate can be determined concomitantly. By assuming that a pure shear stress occurs during shear punch deformation, the average shear stress τ can be related to the force F using the Eq. 1.1:

$$\tau = F/(2\pi rt) \tag{1.1}$$

where t is the specimen thickness and r is the average of the punch and die radii.

3. Results

3.1. Coating Characterization

Cross sections of the resulting as sprayed coatings of 100% CP-Ti and 100% Ti6Al4V are shown in **Fig. 3**. As can be seen, the porosity in the as-sprayed Ti6Al4V coating, which was measured quantitatively by image analysis as 6.7%, is considerably higher than that of the CP-Ti, which is 2%.

The following mixed powders were mixed by weight in a ball mill and then cold sprayed using the same conditions as the single component coatings. Figure 4 shows the effect of adding 10% CP-Ti to Ti6Al4V and 10% Ti6Al4V to CP-Ti. Clearly, these additions have significantly reduced the porosity of the 'matrix' powders; the porosity of the Ti6Al4V has been reduced to 1.5% whilst the CP-Ti porosity is more or less zero. In both cases, there is some evidence that the porosity decreases from the outer surface of the coating to the substrate/coating interface.

In order to examine the effect of powder mixing on the porosity of Ti6Al4V more quantitatively, the level of CP-Ti additions was varied from 5% to 50%.

As can be seen in **Fig 5.a**, 5% of CP-Ti added to Ti6Al4V does not reduce the porosity as much as a 10% CP-Ti addition (**Fig 5.b**). However, adding levels of CP-Ti greater than 10% leads to no further reductions in porosity, e.g. 20% CP-Ti addition shown in **Fig. 5c**. Essentially, additions of 10% of either Ti6Al4V to CP-Ti, or vice versa, leads to a significant decrease in porosity, but little change occurs with increasing levels of CP-Ti added to Ti6Al4V.

The etched coatings are shown in **Fig. 6**. The grey area is Ti6Al4V (arrowed blue), the white and the darker area is CP-Ti (**Fig. 6.a**). In **Fig. 6.a**, there appears to be three phases: the grey

phase and 2 etching phases (red). The darker of the two etching phases appears to have a substructure, which is probably making this structure, look the darker of the two. This could be an etching artefact. As well, the etching of the cross sections appeared to attack the porosity (arrowed green in **Fig 6.b**), and revealed incomplete particle/particle 'bonding' at the grain boundaries (**Figs. 6.a** and **b**). As can be seen from these figures, many of the Ti6Al4V particles remained spherical, which is an indication of a lack of plastic deformation (**Fig. 6.b**). By contrast, the CP-Ti powders appear to have undergone much more severe plastic deformation compared to Ti6Al4V at **Fig. 6.a**.

4. Mechanical Properties

The hardness of the as-sprayed coatings as a function of mixing ratio is plotted in **Fig. 7**. Increasing Ti6Al4V increases the hardness upto 70% at which point there is a small plateau and then a drastic decrease at 95% and 100% Ti6Al4V. This drop is probably related to the higher amount of porosity in these two specimens, although all the microhardness values may be affected by porosity (Ref 13, 14).

Figure 8 shows the τ vs reduction in area (RA) curve of static shear punch tests of the mixed coatings. The static speed was 0.01 mm/sec and the tests were performed only for 10, 70, 80. 90 and 95 % Ti6Al4V content samples. It was observed that there are two types of flow curve obtained regardless of their absolute values, as illustrated schematically in **Fig. 8**. Type 1, **Fig. 8.a**, shows normal 'continuous' work hardening behavior; type 2, **Fig. 8.b**, exhibits an acceleration of work hardening after an initial relatively slow work hardening stage and a lower amount of ductility after reaching the maximum strength . For the as sprayed condition, type 1 is exhibited by the 80, 90 and 95% Ti6Al4V specimens. **Figure 8.c** shows the effect of

composition on the absorbed energy, i.e. the area under the curves of **8.a** and **8.b**. The absorbed energy does not change significantly until 90% Ti6Al4V, at which point the absorbed energy drops drastically.

5. Discussion

5.1. Effect of mixing on porosity

The results indicate that mixing metal powders can have positive effects on the porosity of the single component coatings (**Fig. 9**), with relatively small additions of either Ti6Al4V to CP-Ti, or vice versa, leading to significant decreases in porosity. This diagram also indicates three regions of very low, medium and very high porosity, which correspond to three different mechanisms affecting porosity, as will be explained below.

For a given powder and cold spray equipment, increasing the powder velocity by increasing the gas pressure and velocity and/or changing the gas will inevitably decrease porosity. This is because porosity is a mainly a function of the degree of plastic deformation of the powders and increasing powder velocity translates to increasing plastic deformation. Plastic deformation is basically a way to move material and another way to do this is to move the material at the atomic level by diffusion. Whilst it is true that very high temperatures could be attained locally through adiabatic deformation, the heat is dissipated too rapidly for diffusion to make any impact on the reduction of porosity in cold spray. Therefore, plastic deformation remains the main mechanism to reduce porosity. Thus, the effect of mixing on porosity can then be discussed in terms of considering how differences in size, mechanical properties and morphology could lead to increases in plastic deformation and/or particle velocity.

There is some speculation in the literature regarding the possibility of an optimum particle size distribution favorably influencing porosity by optimal particle packing. For example, Blose (Ref 15) suggests that an observed improvement in consolidation metrics for Ti powders may be correlated to an increased fraction of fines, which could lead to an overall improvement of packing of the powder in question analogous to very small atoms occupying interstitial sites in unit cells of crystals (**Fig. 10**). This generally suggests that packing can be a factor when there is a bimodal distribution of powders with two very different powder sizes. However, in this work, the powder sizes and morphologies of both powders were very similar so the influence on porosity cannot be explained on this basis.

As shown in **Fig. 9**, the effect of composition on porosity can be divided into three regions; the presence of these three regions can be explained on the basis of the difference in hardness between the two types of powder, 141Hv and 385 Hv for CP-Ti and Ti6Al4V, respectively.

The region exhibiting the lowest amount of porosity, which is due to the addition of a small amount of Ti6Al4V to CP-Ti, is labelled 'tamping' because it is probably due to the tamping effect of Ti6Al4V. In a multilayer coating, tamping is the 'hammering' effect on previously deposited layers due to the spraying of subsequent layers. If some harder particles are added to a softer powder, then it may be possible that the harder particles impart an increased intensity of tamping because the kinetic energy of the harder particle would be mainly absorbed by the softer particles and would be converted into plastic deformation. Thus Ti6Al4V additions to CP-Ti can reduce porosity in this way. However, using the same arguments above, the addition of some softer particles to a harder powder is unlikely to improve tamping intensity.

Adding a powder with a difference in hardness can certainly lead to different plastic deformation characteristics. One obvious effect is that the deformation generated between the two particles of different hardnesses may be higher than that generated due to interaction of the same particle species. This is implied in closer observations of the cold sprayed CP-Ti/Ti6Al4V composites, where a decrease in the amount of CP-Ti has led to a higher level of deformation of the CP-Ti (**Fig. 11**). It may be that the heavily deformed CP-Ti forms a continuous network, effectively becoming the matrix, as suggested in the 50% micrograph. This continuous network could reduce the porosity, and this concept can be used to explain the region of mid-level porosity. Thus the region of medium porosity is labelled 'continuous network', with the continuous network being CP-Ti.

Returning to the concept of tamping, the reduction in porosity is fundamentally due to tamping a coating which has a continuous network of CP-Ti. As can be seen from **Fig. 9**, tamping is not effective at Ti6Al4V levels above 50%, even though there is a continuous network of CP-Ti. This is probably because the Ti6Al4V in the coating is absorbing the tamping energy. Therefore, it is likely that the tamping effect will influence porosity at lower than 50% Ti6Al4V, but this 'critical amount' of Ti6Al4V

Finally, the region of highest porosity corresponds to a composite in which the matrix, i.e. continuous network is Ti6Al4V. This is applying the concept, which was used to explain the medium porosity region, that the porosity in mixed powders adopts the porosity of the single component powder which forms the continuous network.

Thus to summarise, there are two mechanisms at play, one to do with tamping and the second to do with establishing a matrix or continuous network. Tamping is effective when there is a

relatively small amount of the harder particles acting on a large volume of the softer material; otherwise the porosity of a mixture is the porosity of the metal that has formed the matrix, or continuous network, in the mixture.

The above mechanisms can also explain how relatively small additions (e.g. 10% by weight) can significantly influence porosity. With regard to tamping, an explanation of the influence of one 'incoming' hard particle could be on the basis of 'nearest neighbors'. For example, if the consolidation of cold sprayed particles can be considered as being analogous to the close packing of spheres of equal size, then each sphere touches nine other spheres as seen in **Fig. 12**. With regard to tamping, by using the nearest neighbor concept, it is obvious that the impact of one hard particle can influence more than one particle. For the 'continuous network' concept, it is clear that far less than 51% of CP-Ti is required to form a continuous network of CP-Ti. Note that above at 10% CP-Ti, the porosity is the same as that of the 100% CP-Ti coating and that there is no further decrease in porosity with increasing levels of CP-Ti to 50%. This suggests that porosity of these specimens is limited by the porosity of CP-Ti, however tamping can further reduce the porosity to below the levels of 100% CP-Ti.

5.2. Effect of mixing on mechanical properties

It is generally accepted that porosity will strongly affect mechanical properties. Therefore, the effect of porosity on hardness and shear punch stress is shown **Fig.13**. At first glance, there appears to be two populations, one associated with low porosity (below 3%), and a much smaller population with about 6% porosity. The higher porosity population clearly has a much inferior set of mechanical properties, which supports the general acceptance that porosity is detrimental. However, in the lower porosity population, there seems to be an indication that increasing

porosity increases the mechanical properties. In fact, this is probably a coincidence with the reality being that this trend is actually related to increasing Ti6Al4V, as was shown in **Fig. 7** where hardness increases with Ti6Al4V until the porosity exceeds a certain level. This implies that the effect of porosity at low levels of porosity, in this case below 3%, is overcome by any changes in composition. Therefore, in general, the effect of porosity below 3% on mechanical properties should be random; this is supported by the value of hardness illustrated by CP-Ti, which has lowest hardness but not the lowest porosity.

6. Conclusions

First and foremost of all, mixing powders generate very interesting composites, which can help explain cold spray mechanisms. Also it can improve the cold sprayability by decreasing porosity. Very low porosities lead to improved mechanical properties. Hardness differences between the two powders are considered to be the first order influence on porosity.

Acknowledgements

The authors acknowledge the McGill Engineering Doctoral Awards and the Natural Research Council of Canada for provision of funding, as well as the Canadian Foundation for Innovation, which funded the McGill-NRC Cold Spray Facility.

References

1. M. Grujicic, C.L. Zhao, W.S. DeRosset, and D. Helfritch, Adiabatic shear instability based mechanism for particles/substrate bonding in the cold-gas dynamic-spray process, *Materials & Design*, 2004, 25(8), p. 681-688
2. A. Papyrin, V. Kosarev, S. Klinkov, A. Alkimov, and V. Fomin, Chapter 5 - Current status of the cold spray process, *Cold Spray Technology*, Elsevier, 2007, p. 248-323.
3. A. Rezaeian, E. Irissou, R. Chromik, and S. Yue, Characterization of cold-sprayed Ni, Ti and Cu coating properties for their optimizations, *Thermal Spray: Crossing Borders*, 2008, p. 2-4

4. J. Sun, Y. Han, and K. Cui, Innovative fabrication of porous titanium coating on titanium by cold spraying and vacuum sintering, *Materials Letters*, 2008, **62**(21–22), p. 3623-3625

5. S.H. Zahiri, Mayo, Sheridan C., and M. Jahedi, Characterization of Cold Spray Titanium Deposits by X-Ray Microscopy and Microtomography, *Microscopy and Microanalysis*, 2008, **14**(03), p. 260-266

6. E. Irissou, J.-G. Legoux, B. Arsenault, and C. Moreau, Investigation of Al-Al2O3 Cold Spray Coating Formation and Properties, *J Therm Spray Tech*, 2007, **16**(5-6), p. 661-668, in English

7. S.H. Zahiri, C.I. Antonio, and M. Jahedi, Elimination of porosity in directly fabricated titanium via cold gas dynamic spraying, *Journal of Materials Processing Technology*, 2009, **209**(2), p. 922-929

8. R. Dykhuizen, and M. Smith, Gas dynamic principles of cold spray, *J Therm Spray Tech*, 1998, **7**(2), p. 205-212

9. T. Marrocco, D.G. McCartney, P.H. Shipway, and A.J. Sturgeon, Production of titanium deposits by cold-gas dynamic spray: Numerical modeling and experimental characterization, *J Therm Spray Tech*, 2006, **15**(2), p. 263-272, in English

10. E. Sansoucy, P. Marcoux, L. Ajdelsztajn, and B. Jodoin, Properties of SiC-reinforced aluminum alloy coatings produced by the cold gas dynamic spraying process, *Surface and Coatings Technology*, 2008, **202**(16), p. 3988-3996

11. B. AL-Mangour, R. Mongrain, E. Irissou, and S. Yue, Improving the strength and corrosion resistance of 316L stainless steel for biomedical applications using cold spray, *Surface and Coatings Technology*, 2013, **216**(p. 297-307

12. R.G. Maev, and V. Leshchynsky, Introduction to Low Pressure Gas Dynamic Spray: Physics and Technology, John Wiley & Sons, 2009.

13. D. Goldbaum, J. Ajaja, R.R. Chromik, W. Wong, S. Yue, E. Irissou, and J.-G. Legoux, Mechanical behavior of Ti cold spray coatings determined by a multi-scale indentation method, *MSA Materials Science & Engineering A*, 2011, **530**(p. 253-265, in English

14. D. Goldbaum, J.M. Shockley, R.R. Chromik, A. Rezaeian, S. Yue, J.-G. Legoux, and E. Irissou, The Effect of Deposition Conditions on Adhesion Strength of Ti and Ti6Al4V Cold Spray Splats, *J Therm Spray Tech Journal of Thermal Spray Technology*, 2012, **21**(2), p. 288-303, in English

15. R. Blose, Spray forming titanium alloys using the cold spray process, *Thermal Spray Connects: Explore Its Surfacing Potential*, 2005,

Table 1. Chemical compositions of powders

Powders	Al	V	C	Fe	O	N	H	Si	Ti
CP-Ti	0.01	0.02	0.01	0.12	0.141	0.004	0.005	0.03	bal.
Ti-6Al-4V	6.4	3.9	0.01	0.21	0.12	0.01	0.006	-	bal.

Table 1. Campaign parameters

Campaign	
Coating thickness (mm)	~ 2
Substrate type	1020 CR steel
Substrate dimensions (mm)	76 x 76
PARAMETERS	
Propellant gas	N_2
Nozzle type	MOC24
Gas pressure (Bar)	40 (~ 4 MPa)
Gas Temperature (°C)	800
Gun Traverse speed (mm/sec)	300
Stand-off distance (mm)	40
Step size (mm)	2
Powder feed rate (g/min)	20 g/min

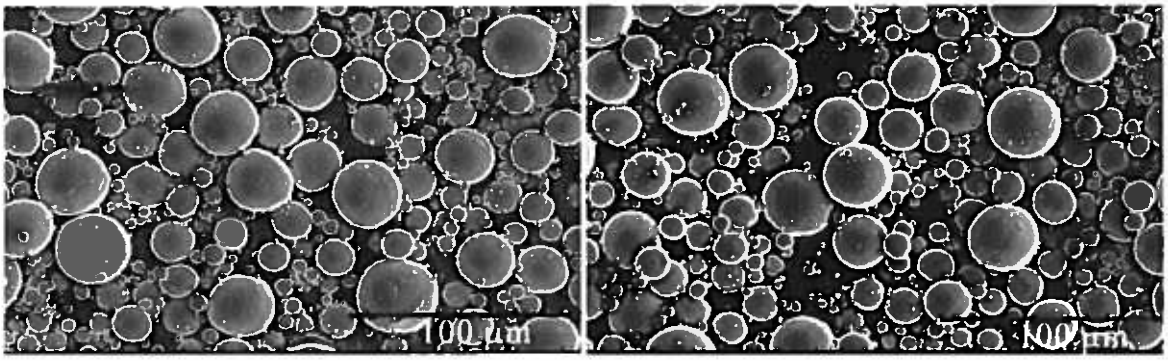

Fig. 1. a) Commercial purity Ti powder and **b)** Ti6Al4V powder

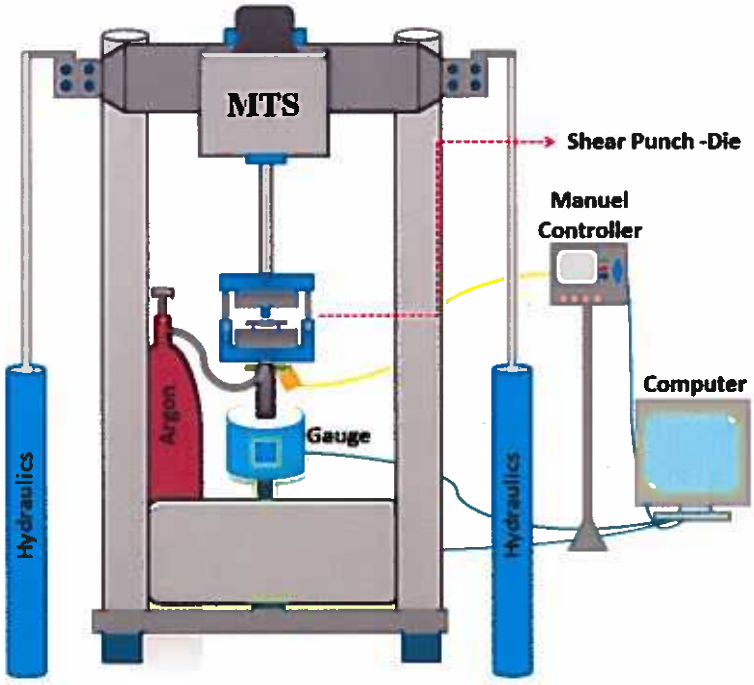

Fig. 2. Schematic of the shear punch testing equipment

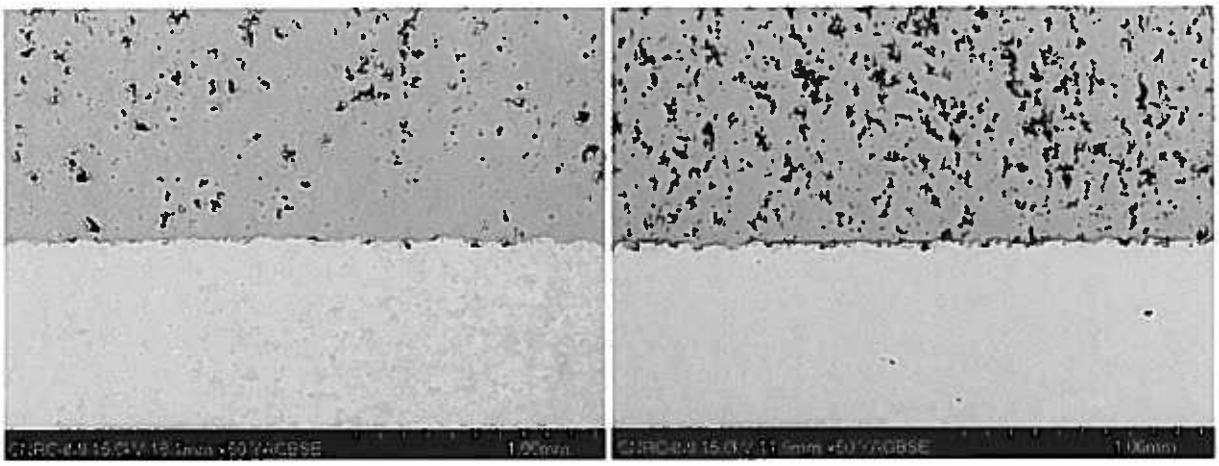

Fig. 3. As sprayed images of **a)** CP Ti and **b)** Ti6Al4V

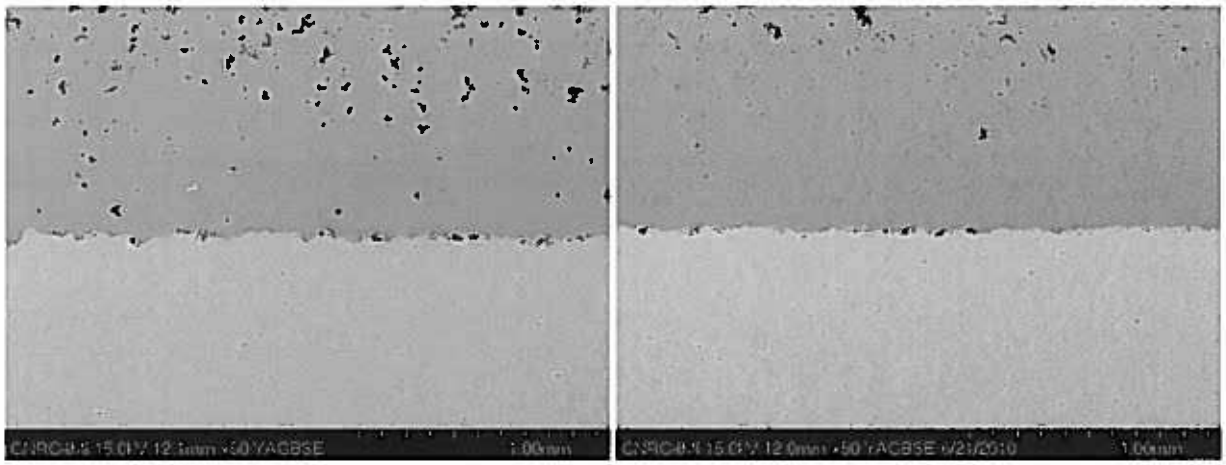

Fig. 4. a) Ti6Al4V + 10% CP Ti and **b)** CP Ti + 10% Ti6Al4V

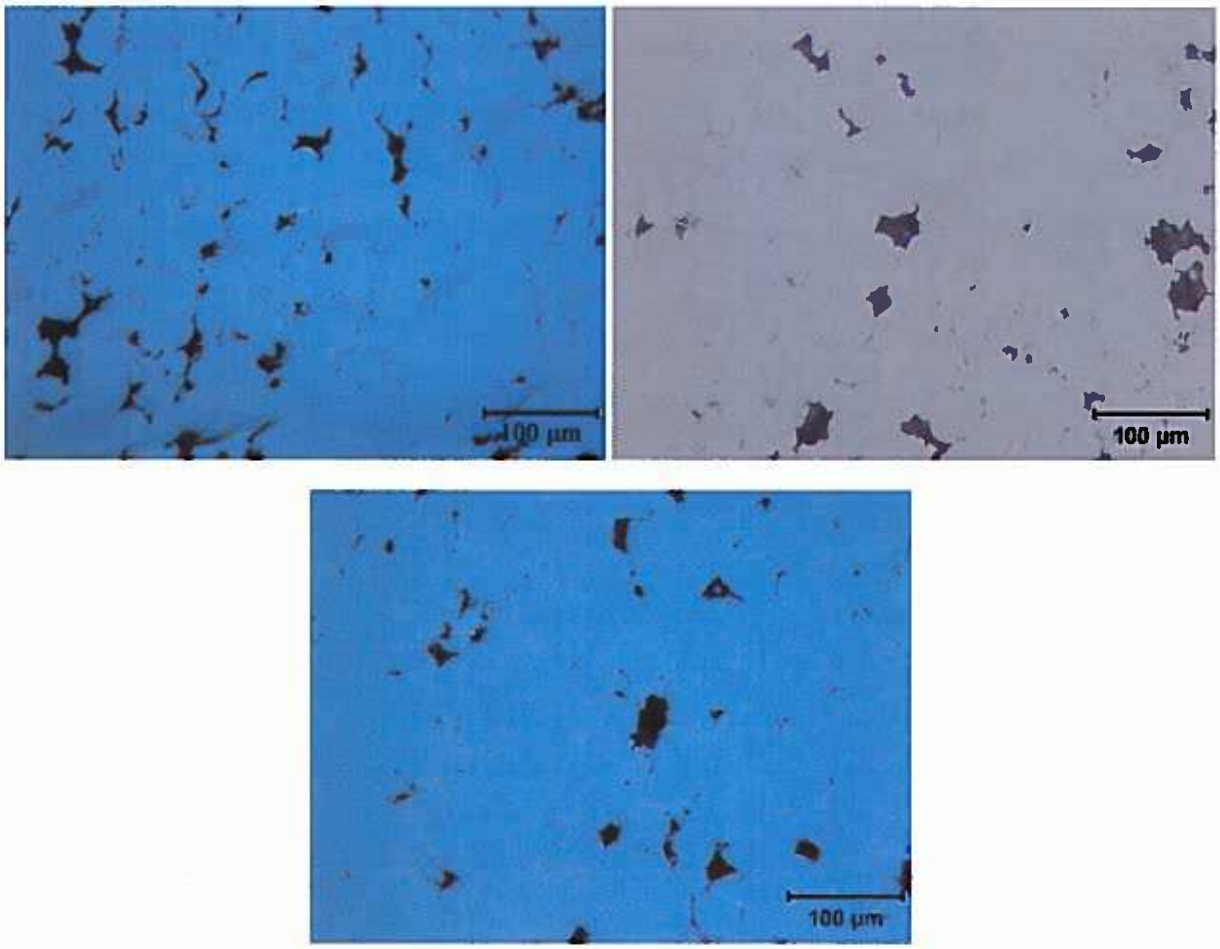

Fig. 5. a) 95% Ti6Al4V + 5% CP Ti, **b)** 90% Ti6Al4V + 10% CP Ti and **c)** 80% Ti6Al4V + 20% CP Ti

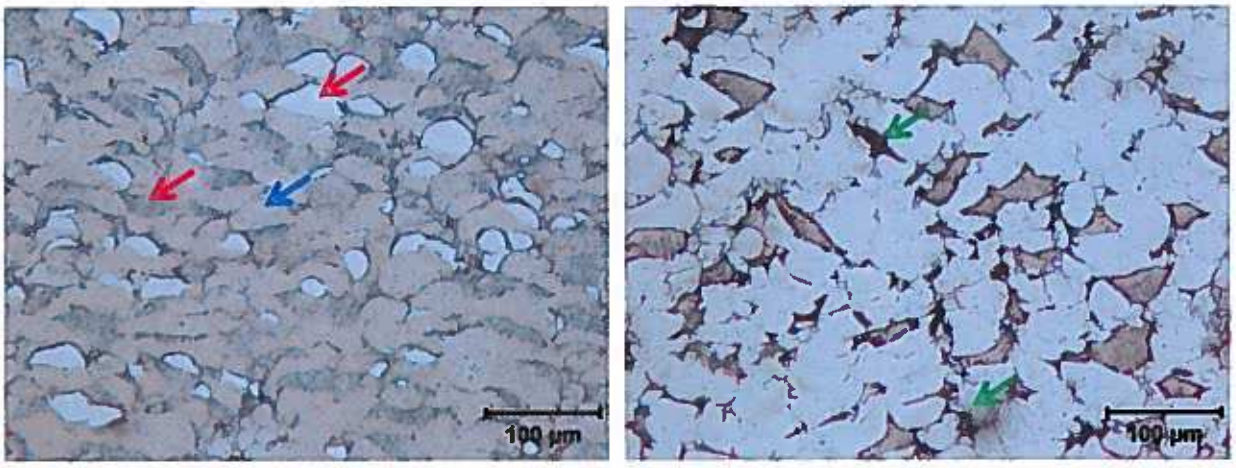

(a) (b)

Fig. 6. The cross section optical images of coatings after etching; **a)** Ti6Al4V + 10% CP Ti and **b)** CP Ti + 10% Ti6Al4V

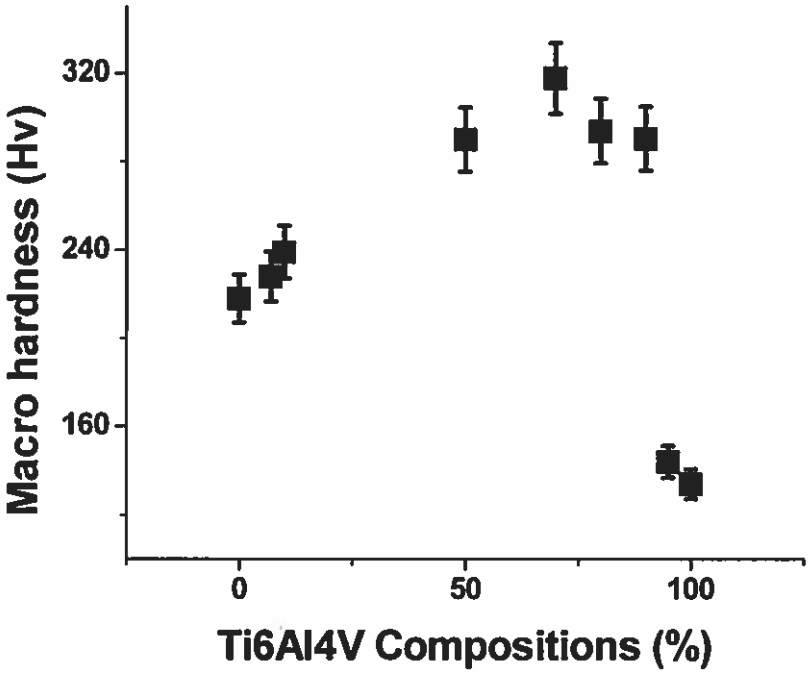

Fig. 7. Macro hardness of samples as a function of Ti6Al4V content

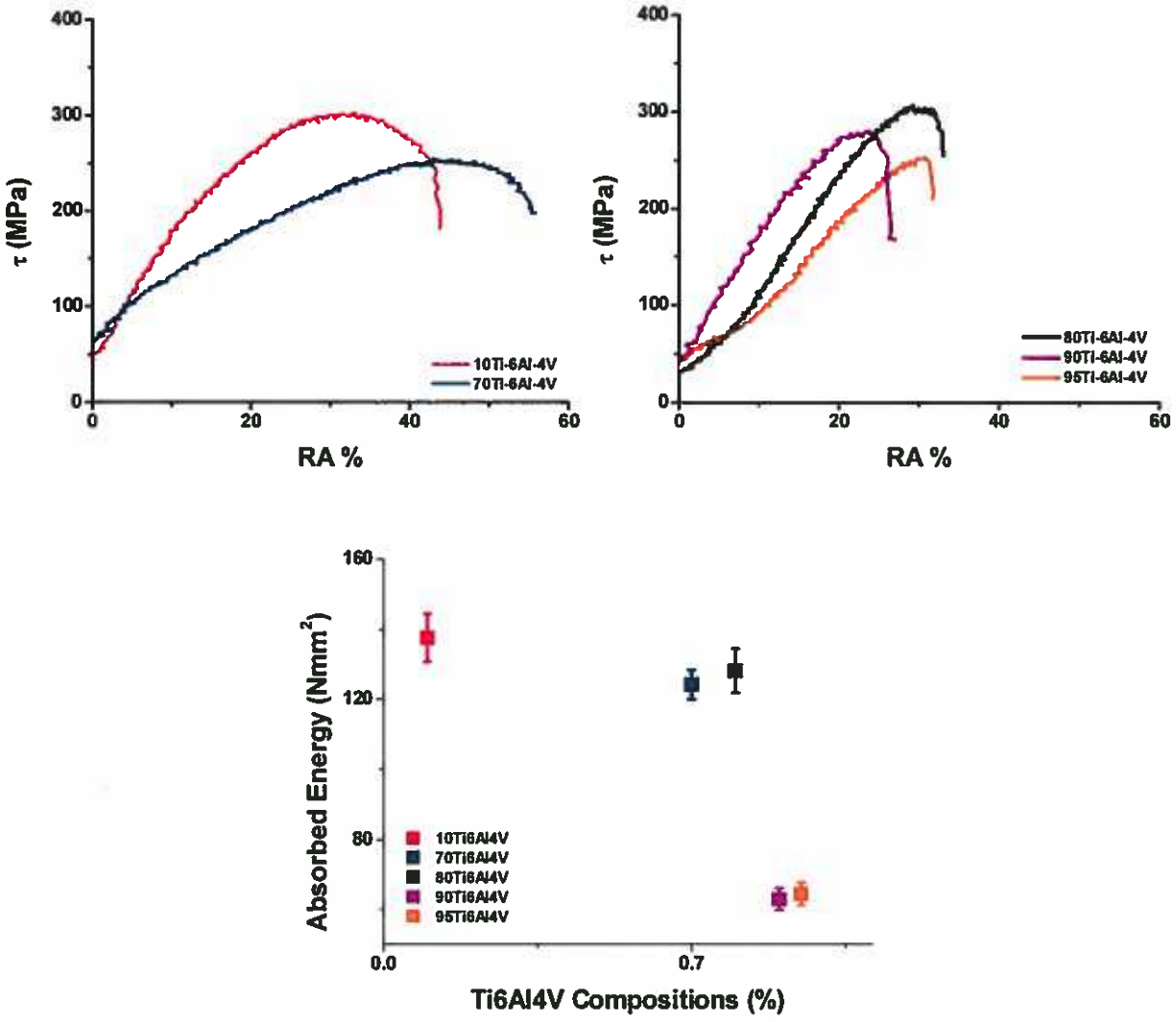

Fig. 8. The force displacement curves of as sprayed coatings **a)** type 1, **b)** type 2 and **c)** absorbed energy vs composition TiAl6V4 after shear punch tests

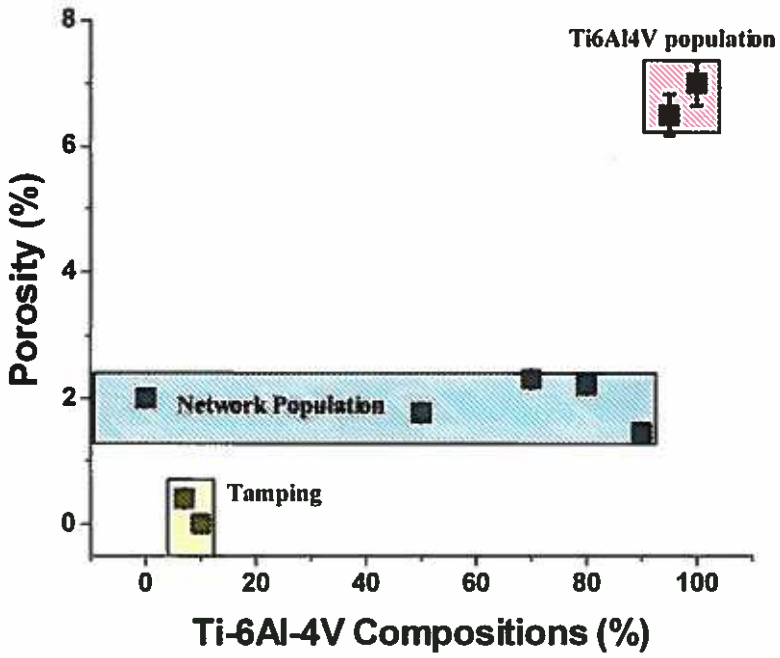

Fig. 9. Effect of mixing Ti6Al4V and CP Ti on porosity. The bars show that adding 10% of CP-Ti or 10% Ti6Al4V decreases the porosity of Ti6Al4V and CP Ti, respectively.

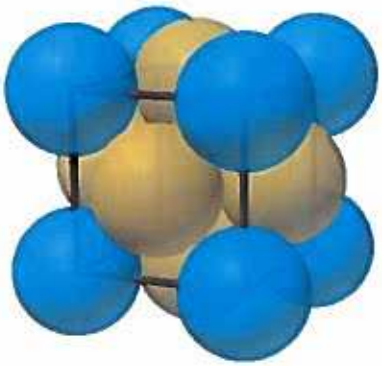

Fig. 10. Interstitial atoms occupying tetrahedral interstitial sites in a close packed structure

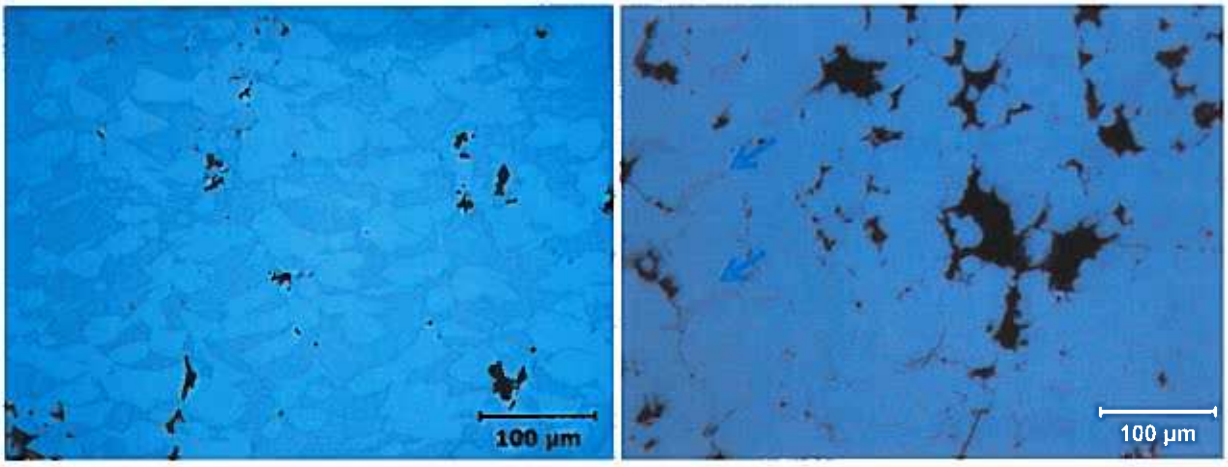

Fig. 11. Mixed CP Ti and Ti6Al4V powder **a)** % 50Ti6Al4V and **b)** %10 Ti6Al4V; the darker phase is CP Ti. The decrease from 50% to 10% CP Ti has led to a much increased deformation on the CP-Ti.

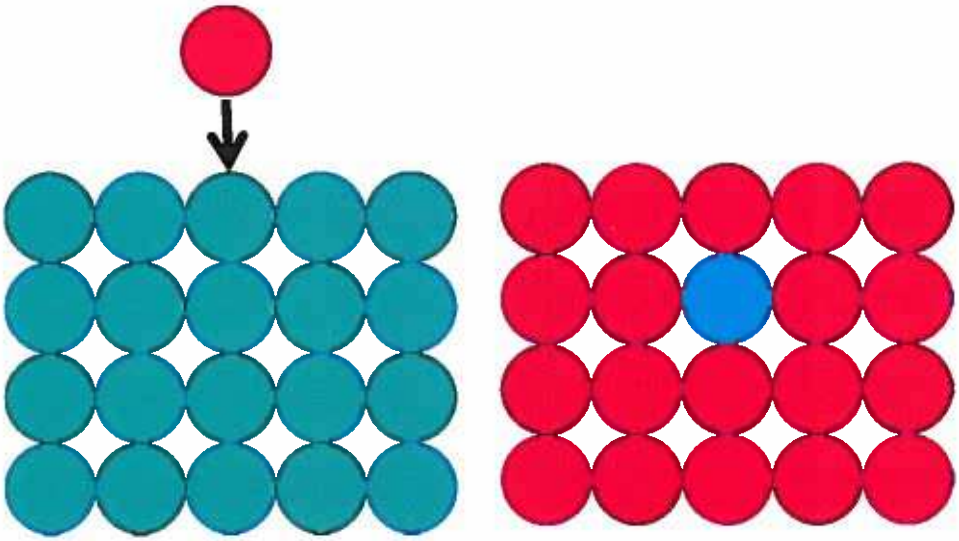

Fig. 12. Effect of mixing Ti6Al4V and CP Ti on porosity

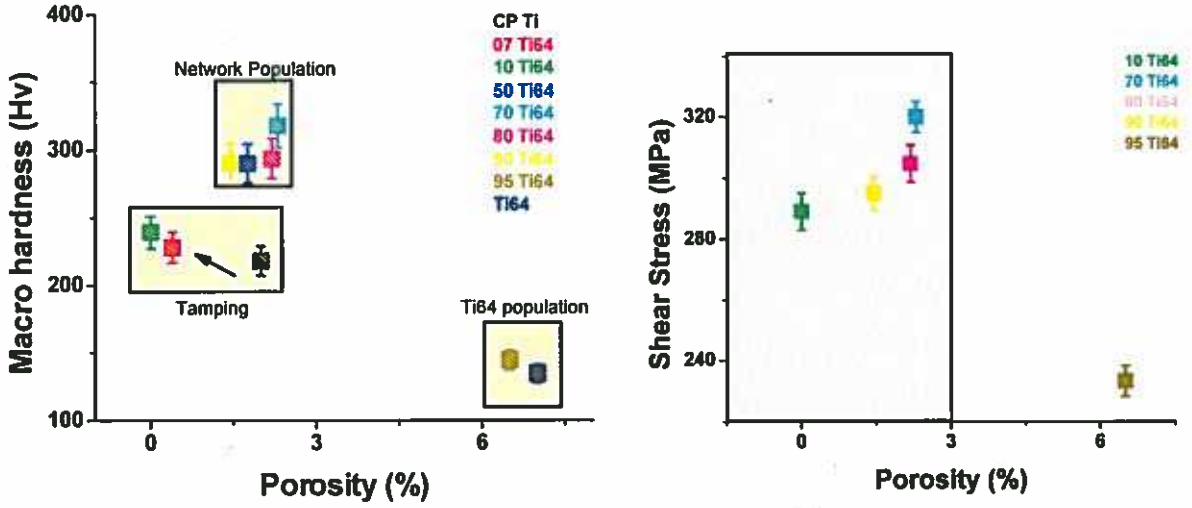

Fig. 13. **a)** Macrohardness and **b)** Shear stress as a function of porosity